Systematic trends of first-principles electronic structure computations of $Zn_{1-x}A_xB$ diluted magnetic semiconductors

R. D. McNorton, T. M. Schuler, and J. M. MacLaren
Department of Physics, Tulane University, New Orleans, Louisiana 70118, USA

R. A. Stern
Seagate, 7801 Computer Avenue, Bloomington, Minnesota 55435, USA

(Received 27 March 2008; revised manuscript received 13 June 2008; published 26 August 2008)

This paper presents a study of the calculated electronic properties of the Zn-based II–VI dilute magnetic semiconductors in a $Zn_{22}A_2B_{24}$ structure, where A=Cr, Mn, Fe, Co, and Ni, and B=S, Se, and Te. In this study we investigate the local densities of states of the magnetic ions and host semiconductor, the magnetic exchange interactions as a function of transition-metal ion separation and orientation, the origins of the magnetic coupling, the tendency for impurity atoms to cluster creating impurity rich regions—at least thermodynamically, and the local magnetic moments. The results show half-metallic behavior for Cr, Fe, and Ni impurities, and in the case of Cr and Ni a ferromagnetic coupling consistent with the double-exchange mechanism. The Mn- and Co-doped materials are found to be semiconducting and couple antiferromagnetically, which can be explained by the superexchange model. The Fe-doped materials show the sign of the coupling is dependent on the orientation and separation of the impurities.

DOI: 10.1103/PhysRevB.78.075209 PACS number(s): 75.30.Et, 75.50.Pp, 71.20.−b, 31.15.A−

I. INTRODUCTION

Semiconductors containing small amounts of magnetic impurities, known as dilute magnetic semiconductors (DMS), have been of interest to the physics and engineering communities for quite some time.[1–3] The intriguing, and potentially technologically useful, property that arises out of these materials is the possibility of strongly spin polarized currents. This is electronically possible when either the majority or minority-carrier states dominate at the Fermi energy. In the extreme case of half-metallic materials, one spin channel is conducting while the other spin channel is strictly insulating.[4] It is this idea of spin polarized currents that would allow engineered devices that combine the properties of magnetism with the traditional semiconductors to create the so-called spintronic devices.

The electronic structure of the material depends on the particular host crystal structure and on the magnetic impurity atom. The particular DMS compounds studied here have crystal structures in which the bonding interactions occur between the semiconductor *s-p* orbitals and the magnetic ion's *d* orbitals. The nature of this bonding determines the physical properties observed in our calculations. It has been suggested[1,5] that one of the variables determining the strength of the exchange interactions is the amount of *sp-d* hybridization between the host and impurity. To this end, we have studied in detail the electronic structure of wide band gap II–VI semiconductors ZnS, ZnSe, and ZnTe, which form in the zincblende structure and contain the magnetic impurities Cr, Mn, Fe, Co, and Ni.

Prior work has confirmed that the II–VI compounds doped with Cr are ferromagnetic[5–9] (FM) even at room temperature, however they require a high concentration of the Cr impurity.[10–12] Mn-doped systems have been studied extensively due to the giant Zeeman splitting of the *d* bands. This splitting results in Mn being easy to model and study due to a small number of exchange mechanisms being possible. Mn has been predicted and observed experimentally to have an antiferromagnetic (AFM) coupling via the superexchange.[2,13–15]

Compounds containing Fe impurities, with their magnetically inactive singlet ground state (GS), have been shown to be AFM,[13] FM,[16] and spin-glass[7] compounds. These differing results indicate that the magnetism in Fe DMS compounds is frustrated which is manifested through a competition between exchange mechanisms. Ni-doped systems have also been shown to be FM (Ref. 5) and AFM (Refs. 6 and 7) and Co-doped systems have been determined to be AFM in nature.[5–7,17] These studies show hybridization between the impurity's *d* shell and the *p* shell of the near neighbor anion. The short range of the *d* orbital prevents any other significant hybridization between more distant neighbors to occur.[15] The hybridization between these orbitals is greatest in Cr, followed by Ni and Fe. All of these materials have been found to be half-metallic.[5] The results of a similar study for ZnCrTe are consistent with the data presented here, and suggest that in determining the exchange properties of the DMS structures one must take into account both the impurity separation and bonding direction between the impurities and the anions.[18] This is to be expected since the mechanisms behind the magnetic coupling are the double-exchange (DE) and superexchange (SE) processes.

In this paper we will further develop the results of a prior work[5] which found that Cr and Ni impurities in the semiconductor ZnX (X=S, Se, Te) result in a FM coupling, with Cr producing the stronger coupling of the two, while Mn and Co impurities yield an AFM GS. The DE mechanism, presumably, is responsible for the ferromagnetism observed in the former compounds. Compounds containing Fe impurities produce a half-metallic state and thus are able to participate effectively in a DE process via the conduction band (CB), but do not exhibit a FM GS except at certain transition-metal (TM) separations and orientations.

It will be shown that the filling of the TM *d* states and the orientation of the TMs to one another determines which *d* orbitals participate, the amount of *p-d* hybridization, and thus the exchange coupling. The ability or ease in which electrons can hop through the crystal given the particular atomic arrangement and density of states appears to be another contributing factor to the sign and strength of the exchange coupling. While the SE mechanism is an indirect exchange mediated by the *p* orbital of the group VI element,[2] we propose that in certain circumstances a DE coupling[19] can occur which we suggest explains the observation of a FM alignment. We postulate that the two exchange mechanisms can be in competition and the one that is favored is determined by fundamental factors of the electronic structure, the magnetic ion orbitals which are involved, and the separation distance between the impurities.

To gain an understanding of the effects of a random distribution of impurities, which would occur in real samples, we have calculated the densities of states (DOS) and exchange energies for a variety of impurity-impurity separations and orientations. The calculation of the GS energies for various impurity separation distances suggests that there is a tendency of these implanted ions to cluster together. The spatial distribution of the magnetic impurities in the host is clearly important in determining the magnetic properties of these materials. Obtaining experimentally an atomic distribution of magnetic impurities in a real sample is a difficult task, and one would expect that since there is a thermodynamic tendency to cluster that there will be regions that are impurity rich as well as regions that are impurity poor. Such composition fluctuations affect the electronic structure and magnetic coupling of the system. The distribution of impurities has a significant effect in the cases where SE is the dominant mechanism. Anderson[20] showed that the SE interaction was determined by the interatomic transfer integral between *p-d* wave functions

$$\frac{2J}{k_bT} = \frac{2b^2}{4S^2U}, \tag{1}$$

where J is the interaction energy between magnetic ions, $2S$ represents the number of unpaired electrons, U is the energy required to add an extra electron to a neutral solid (electron affinity), and b is the transfer integral. It has been previously shown that $b \propto d^{-8}$, where d is the spacing between impurities.[21]

A. Zincblende II–VI DMS

The II–VI DMS materials have been studied extensively, in part owing to the fact that their band gap, lattice constant, and other band parameters can be tuned by varying the ionic composition.[2] This property could make these II–VI's potentially useful for a wide range of electronic applications and has also been observed in III–V DMS materials.[22] The structure of these materials is that of zincblende for ZnS, ZnSe, and ZnTe when the impurity concentration is 4%,[2] as was determined in this study. It has been suggested that some II–VI materials will form in the wurtzite structure at impurity concentrations above 10%,[2] however these concentrations and structures are not considered in this work. The zincblende structure is derived from a diamond bravais lattice, with *A* and *B* atoms on adjacent sites. Thus each *A* atom has four nearest-neighbor (nn) *B* atoms, and vice versa. This tetragonal symmetry at the atomic sites is important in determining the exchange mechanism between magnetic impurities. The crystal-field effect on a tetragonal site will split the magnetic ion *d* shell into two levels the e_g subshell, which is lower in energy and holds only two electron pairs, and the t_{2g} subshell, which is higher in energy and holds three pairs of electrons.

These materials also exhibit tetrahedral bonding at all lattice sites, which results in sp^3 bonding between constituents. This effect is well known to be maximized in the II–VI semiconductor, owing to the complete filling of valence states. If we introduce impurities into the host the amount of sp^3 bonding will depend on the impurity introduced. In a II–VI semiconductor doped with Mn this bonding strength is maximized, as the Mn half-filled *d* shell can virtually act as a filled valence shell, similar to the cation II element. The Mn atom can thereby replace the cation and still remain virtually as stable as the host semiconductor.[2]

TABLE I. Lattice constants and energy gaps of II–VI semiconductors in the zincblende structure, comparing the DFT calculations with experimental (Ref. 2) measurements.

Material	L_0 (Å)		Energy gap (eV)	
	calc.	expt.	calc.	expt.
ZnS	5.44	5.416	2.88	3.84
ZnSe	5.73	5.670	2.48	2.82 (300 K)
ZnTe	6.09	6.102	1.86	2.39 (300 K)

II. COMPUTATIONAL DETAILS

Supercell computations were performed with the Vienna Ab-initio Simulation Package (VASP),[23] using all-electron frozen-core projector augmented wave (PAW) potentials[24,25] and the generalized gradient approximation (GGA) to the exchange-correlation energy.[26] The GGA functional was that of Perdew-Wang 1991 (PW91) (Ref. 26) using the interpolation of Vosko *et al.*[27] Potentials for all magnetic impurities, except Co, treated the $3p$ and $4s$ semicore states as valence states, while the Co potential treated only $3d$ states as valence states. Energy cutoffs were calculated by converging the GS energy by varying the ENCUT parameter in VASP. They were determined to be 319 eV for the Cr, Mn, and Co systems, 345 eV for the Fe system, and 400 eV for the Ni system. Lattice constants were converged in a manner similar for the nonmagnetic semiconductor hosts. Their values were then used for the DMS computations as indicated in Table I. We did not consider any local lattice relaxations or spin-phonon interactions that may occur around the impurity atom. Calculated and experimental lattice constants and band gaps for pure II–VI semiconductors are given in Table I. The computed lattice constants of the Zn*B* compounds are quite close to the experimental values, although the band gap is significantly under estimated.

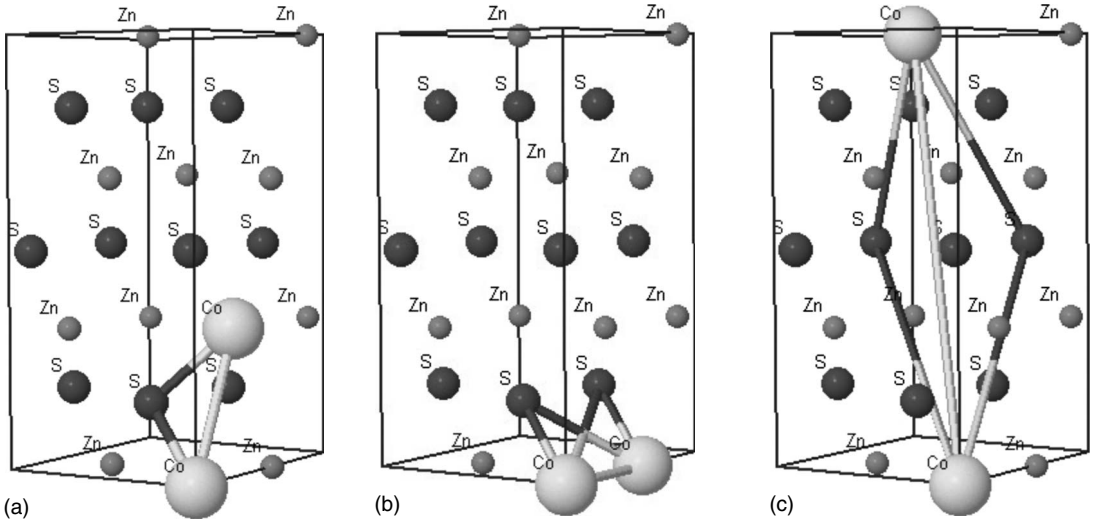

FIG. 1. Atomic arrangement of impurities for three of the six possible supercell configurations. The separation of the impurities in the figure in terms of the lattice constant L_o and are (a) $=.707L_o$, (b) $=1.225L_o$, and (c) $=1.871L_o$, where L_o represents the lattice constant of the undoped semiconducting compound.

The DOS and exchange calculations of the magnetically doped materials were calculated via supercell computations of the materials $Zn_{22}A_2B_{24}$, where B=S, Se, Te, and A=Cr, Mn, Fe, Co, Ni. This corresponds to a TM concentration of roughly 4% for the entire crystal. Each unit cell consisted of eight atoms, and the dimensions of the supercell were 1 unit cell in the x direction, 2 unit cells in the y direction, and 3 unit cells in the z direction. These supercells were constructed to yield either an FM or AFM GS. A $3\times3\times1$ grid for a total of four k points was used to reduce calculation time, while still maintaining a total-energy convergence of better than 1.0 meV/atom for all calculations. Several different spacings of the magnetic impurity were modeled in the calculations in order to represent the possible spacings of the impurities allowed within the zincblende structure. These possible spacings were found to be (from least to greatest, in units of the lattice constant $[L_o]$): $.707L_o$, $1.000L_o$, $1.225L_o$, $1.414L_o$, $1.581L_o$, and $1.871L_o$. The actual ionic positions in the supercell are (0 0 0) for the one impurity that remains fixed, and for the variable impurity the positions (from least separation distance to greatest) are (1/2 0 1/2), (1 0 0), (1 1/2 1/2), (1 0 1), (0 1/2 3/2), and (1 1/2 3/2). For visualization, three of these configurations are portrayed in Fig. 1.

III. ELECTRONIC STRUCTURE

A. DMS DOS

First we will summarize the electronic properties of the pure II–VI semiconductors. The total density of states for zincblende ZnS is shown in Fig. 2. The large sharp peaks at ~-6 eV are the Zn d states which do not hybridize significantly with the group VI anion orbitals. The broad feature between the Zn d states and the Fermi energy (set to 0 eV) is composed of Zn-s and S-p states of bonding. The unoccupied states are also hybridized mixtures of Zn-s and S-p states. The feature at ~-12 eV reflects the S-s states.

The DOS of these DMS materials can be used to study trends that emerge when the TM ions and their separations are varied, and also determine whether the material is semiconducting or half-metallic. In this study we focus on the effect the TM separation has on the electronic and magnetic properties of the compound.

The total and partial densities of states for different TM impurities at a constant spacing in ZnS are displayed in Fig. 3. In the TM DOS (solid black line) we see that as the impurity increases in atomic number from Cr to Ni the d peaks of both the conduction and valence bands shift down in energy such that the magnetic ion maintains an integer spin moment. For Cr, Fe, and Ni impurities, the d peaks of the TM coincide with the Fermi energy (E_F). For materials containing Mn and Co impurities there are no d states at the Fermi energy. The II–VI materials that contain Cr, Fe, and Ni are therefore determined to be half-metallic, while materials

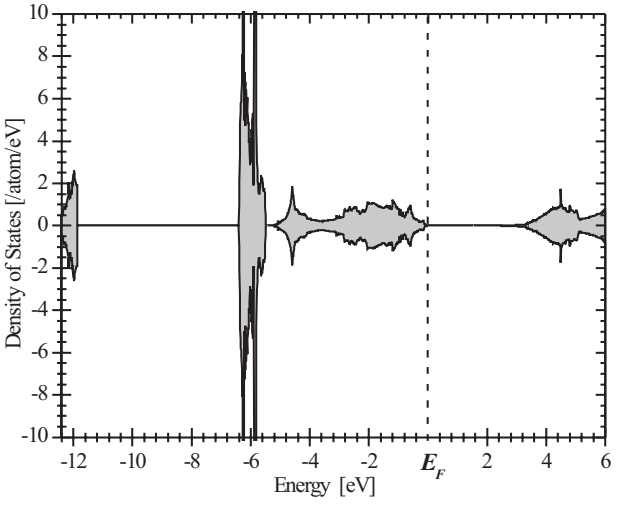

FIG. 2. Spin resolved DOS of zincblende ZnS, with the positive y axis displaying spin-up states and the negative y axis displaying spin-down states.

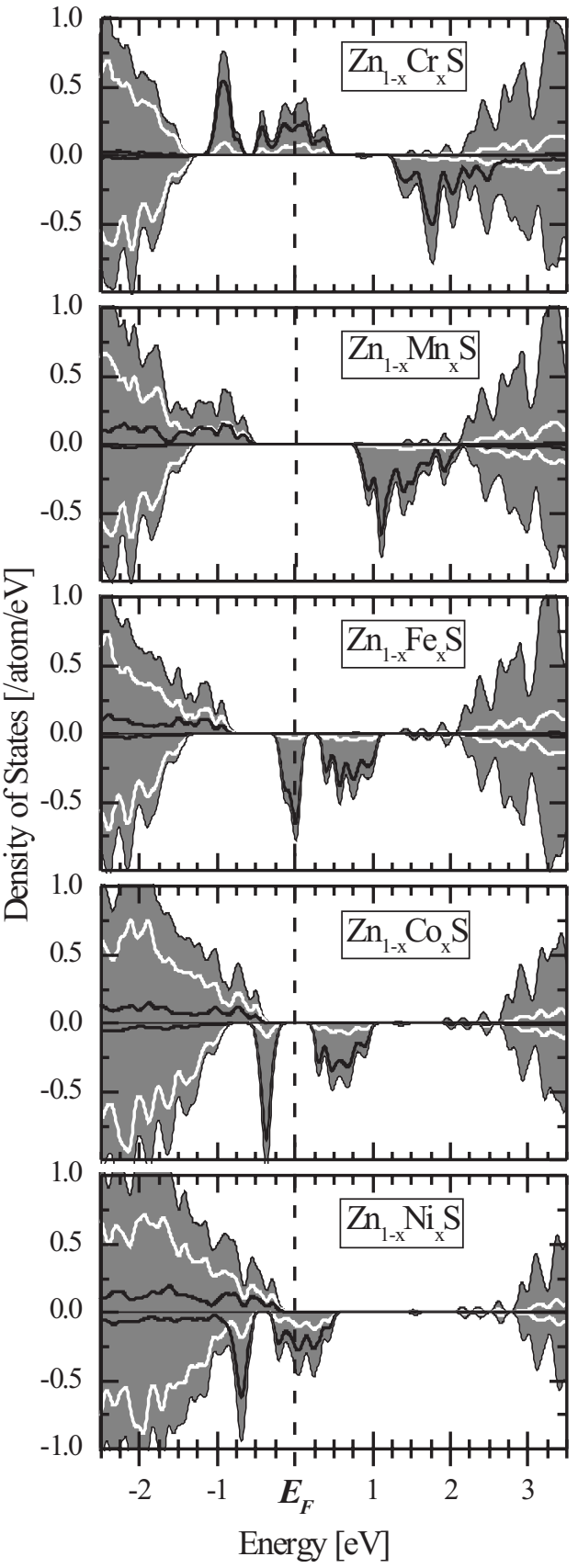

FIG. 3. DOS of Cr, Mn, Fe, Co, and Ni in ZnS, forming a FM DMS. The shaded region is the total DOS, the solid line represents the TM-*d* state, and the white line represents the anion-*p* state.

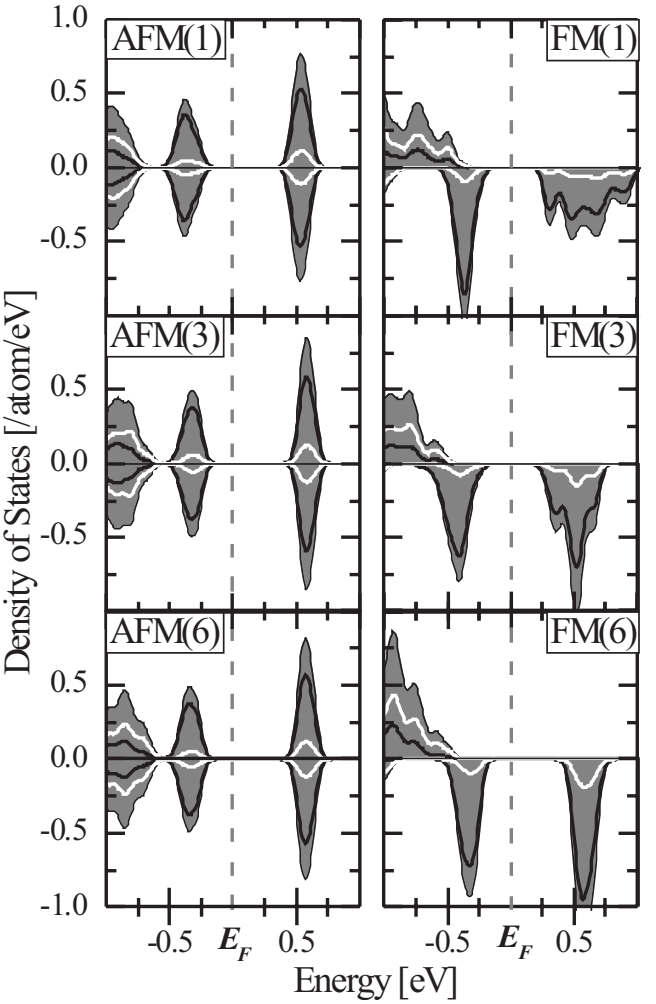

FIG. 4. DOS of ZnCoS in the AFM state (left column) and FM state (right column) for the different crystal impurity spacings, with plots (1), (3), and (6) corresponding to separations of $0.707L_0$, $1.225L_0$, and $1.871L_0$, respectively. The shaded region is the total DOS, the solid line represents the TM-*d* state, and the white line represents the anion-*p* state.

doped with Mn and Co impurities are found to be semiconducting.

Ni and Fe have spin minority carriers at the Fermi energy while Cr shows the presence of spin majority carriers. When the *d* orbitals of the TM impurity lie in the gap of the host semiconductor (SC) we can clearly see the crystal-field (CF) splitting of the *d* band into the e_g and t_{2g} states, which are ordered in the manner expected for an ion in a tetrahedral site. However, as we progress through the TM series, the populated *d* states decrease in energy and hybridize with the host valence band (VB), forming a broad band from which the e_g and t_{2g} suborbitals can no longer be clearly distinguished. This behavior is seen in the DOS for all of the impurities.

By examining one particular impurity (ZnCoS) we can compare changes to the DOS as the impurity spacing is increased (Fig. 4). In the FM ZnCoS DOS (right column of Fig. 4), we see that when the TM impurities get further apart the TM-*d* states become more localized, as expected. This

TABLE II. Energy gap between the occupied and unoccupied orbitals are tabulated from the DOS of the FM alignment for the materials Zn(Cr,Mn,Fe,Co,Ni)(S,Se,Te) using the closest ionic spacing possible ($0.707L_0$).

Spin	ZnCrS ZnCrSe ZnCrTe	ZnMnS ZnMnSe ZnMnTe	ZnFeS ZnFeSe ZnFeTe	ZnCoS ZnCoSe ZnCoTe	ZnNiS ZnNiSe ZnNiTe
		1.75	2.03	2.09	2.09
Majority		1.33	1.48	1.47	1.47
		1.48	1.55	1.71	1.46
	2.39	1.93			
Minority	1.83	1.59		0.19	
	1.27	0.89			

results in a narrowing of the energy spectrum for the TM-*d* state which creates an increased band gap. This is to be expected as when the impurities are placed further apart in the lattice there will be a reduction in *d*-*d* orbital interactions.

In the AFM DOS (left column of Fig. 4) we see that the TM-*d* orbital structure resembles the *d*-orbital peaks in the FM DOS, though having slightly greater splitting. This is due to the fact that in the AFM material, the *d*-*d* interaction between like magnetic spins occurs at larger distances. The only noticeable change between the different impurity separations in this plot is the location of the AFM DOS peaks with respect to the top of the VB. A small repulsive interaction between the occupied *d* states with the states at the top of the VB composed of hybridized *p* orbitals of the anion and *d* orbitals of the TM. The consequence of separating the impurities is that it will further narrow the impurity band, which reduces the repulsive interaction and allows these VB states to move slightly higher in energy, reducing the energy separation between the impurity *d* and valence orbitals from 0.50 to 0.25 eV. This effect is seen in AFM compounds doped with Cr, Co, and Ni impurities, but not Mn or Fe impurities, and it is not observed in the FM case for any of the impurities because the energy separation between the TM-*d* and the spin-down VB states is large.

Table II lists the calculated band gaps for all of the DMS materials discussed in this work, and from this data we see that the half-metals ZnCr*B*, ZnFe*B*, and ZnNi*B* (*B*=S, Se, Te) have a small gap between the valence and conduction bands within the semiconducting channel. The AFM oriented states of Mn exhibit a band gap that ranges from 0.86 to 1.46 eV. Likewise, the Co DMS have a range between 0.28 and 0.412 eV. By comparing these values to the calculated band gaps of the host semiconductors (from Table I) we see that, with the introduction of the impurity, the band gap generally decreases as the number of occupied electron shells within the anion increases. This effect is evident when we plot the DOS of the TM *d*-majority-spin states for each potential anion of increasing atomic number, as is shown for Ni impurities in ZnS, ZnSe, and ZnTe in Fig. 5. With the introduction of the greater number of occupied electronic shells associated with there is a broadening of the VB orbitals resulting in a smaller band gap. Experimentally it is found that increasing the concentration of the impurity would result in an increase of the band gap, especially in Mn.[2]

One property of half-metallic materials is that the TM ion should exhibit integer spin moments, which is confirmed in all of our calculated half-metallic systems. In conjunction with the DOS, this would suggest that the hybridization between the anion *p* shell and the TM *d* states preserves the total integer moment of the TM, and the spin moment is preserved because the exchange splitting of the TM is greater than the CF splitting, which ensures the filling of electron shells according to Hund's rules. Though the CF splitting is sufficient to separate the e_g and t_2g states, the subbands show some of their own structure, particularly in the case of the t_{2g} which shows apparent hybridization with the host states. One reason for the increased hybridization of the t_2g states is that these orbitals are oriented diagonally between the crystal axes (d_{xy}, d_{zx}, and d_{yz}).

The integer moments of each impurity correspond to the accepted free moments of the TM ions, which are 4(Cr), 5(Mn), 4(Fe), 3(Co), and 2(Ni). The lone exception is that of ZnNiTe, where the Ni ion exhibits a maximum of 0.25 μ_b reduction in the magnetic moment, representing a 12.5% re-

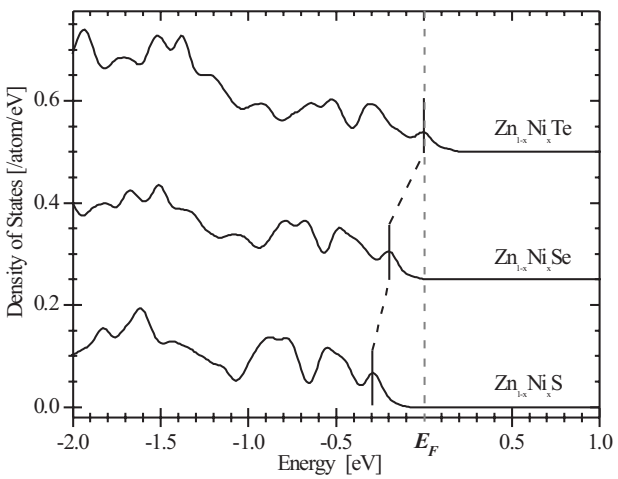

FIG. 5. DOS of the Ni-*d* VB for ZnNiS, ZnNiSe, and ZnNiTe are plotted to show the broadening of the VB that occurs as the size of the anion increases. This broadening is a product of the uppermost valence electrons shifting toward the Fermi energy (0 eV) as indicated by the two vertical lines. The larger electronic bands and increased *p*-*d* hybridization associated with larger anion atoms create this effect.

TABLE III. Calculated values of the partial charge [units of electron charge (e)] and magnetization (μ_b) on the Ni atoms in ZnS, ZnSe, and ZnTe compounds.

Material	s		p		d		Total	
	chg.	mag.	chg.	mag.	chg.	mag.	chg.	mag.
ZnNiS	0.742	0.006	6.903	0.085	8.832	1.208	16.477	1.299
ZnNiSe	0.810	0.008	6.939	0.095	8.941	1.151	16.691	1.254
ZnNiTe	0.927	0.008	7.091	0.103	9.136	0.898	17.154	1.009

duction from the free atom. The moment calculated for the Ni ion in ZnNiTe for each ion separation in the order of least to greatest is 1.75 μ_b (1), 1.825 μ_b (2), 1.85 μ_b (3), 1.86 μ_b (4), 1.93 μ_b (5), and t_{2g} (6). The reason for this is apparent from the partial DOS of the Ni d states in the VB presented in Fig. 5 for our ZnNiS, ZnNiSe, and ZnNiTe systems. As the anion changes from S→Se→Te, there is a definite broadening of the peaks at the locations of both the e_g peaks, which move from −0.60 to −0.30 eV with increasing anion size, and the t_{2g} peaks, which move from −0.40 to 0.00 eV with increasing anion size. Calculations of the partial charges and magnetizations of the Ni atoms in these materials (Table III) show that the Ni ions are gaining charge from their nearest-neighbor anions, and that the amount of charge gained increases with the size of the anion. This would suggest that the sp-d hybridization is greater for the ZnNiTe compound. This hybridization dictates the strength of the SE so ZnNiTe should become more AFM oriented than the S and Se counterparts.

IV. SUPEREXCHANGE VERSUS DOUBLE EXCHANGE IN THE II–VI DMS

Since the magnetic ions are not near neighbors the direct exchange is too weak to explain the size of the exchange coupling observed. However, indirect exchange mechanisms can provide exchange couplings of the right size. In many DMS compounds it is generally believed that Anderson's superexchange[20,28] and Zener's DE mechanism are responsible for the magnetic coupling. One major difference between these two exchange mechanisms is the role of the mediator. In SE the role of the mediator is played by a pair of p electrons of the host anion (S, Se, Te). One p electron is transferred to a neighboring TM while the other directly exchange couples with another neighboring TM ion. This coupling normally reduces the kinetic energy and is FM for d shells that are less than half-filed, and AFM otherwise. The DE process is mediated by the CB of the host crystal via a resonance state that mixes same spin d orbitals of the TM ions and extended CB states. Thus the DE coupling requires an extended metallic state, and since this state couples wave functions of the same spin, the coupling has to be FM.

For a SE mechanism to apply there needs to be a significant p-d hybridization between the anion-p and TM-d orbitals to promote the electron transfer and a small relative energy difference between the p orbital and available d states as would be expected from perturbation theory. Clearly, the requirements for the material to participate in a DE are that the d electron must be able to propagate through the CB and there must be an allowable empty d state to propagate into. It has been often suggested that these two mechanisms are in competition with one another.[17] The following analysis will examine why and which DMS compounds exhibit this competition.

The particular electronic structure of these DMS materials provides a qualitative explanation of which exchange mechanism might be involved. The DMS materials, studied here, doped with either Cr, Fe, or Ni are half-metallic and exhibit a competition between these two exchange mechanisms which can either manifest in a weak coupling (Fe), strong coupling (Cr), or moderate coupling (Ni) of the magnetic ions depending on the relative strengths of the two mechanisms. Those doped with Co and Mn are insulating and therefore expect predominantly exhibit an AFM SE coupling.

Figures 6(a)–6(e) show how the DE mechanism operates. In Mn [Fig. 6(b)] the DE is prohibited and in Co [Fig. 6(d)] is unfavorable. In both cases the compounds are insulating. Mn has no empty majority-spin d orbitals. Therefore the magnetism in Mn DMS compounds is strictly AFM and regulated by the SE. The Co DMS compounds are insulating but have some low lying unoccupied t_{2g} states that could exhibit a weak FM DE.

The three cases of Cr [Fig. 6(a)], Fe [Fig. 6(c)], and Ni [Fig. 6(e)], the half-metallic nature of the electronic structure would permit a FM DE to occur. The Cr DMS compound is half-metallic in the spin-up direction while Fe and Ni are half-metallic in the spin-down direction. Being a half-metal promotes considerable sp-d coupling between the d orbital of the TM and sp orbital of the CB. This coupling will facilitate the transfer of spin between the two neighboring TM-d shells. The exchange splitting is large enough to ensure that the transferred electron is accepted by the incomplete t_{2g} shell of the neighboring TM. For Cr, Fe, and Ni the DE results in either a half-shell (Cr), half-subshell (Ni), or both (Fe) electronic configurations. By maximizing S the ground-state energy is lowered due to guidelines of Hund's rules. The strength of the FM DE for each TM from this analysis in decreasing order is Cr, Ni, Fe, Co, and Mn.

Figures 7(a)–7(e) show how the SE operates either by a FM or AFM coupling. The larger the energy difference between the localized TM d peaks and the p orbitals (VB) and the narrower the d orbital is the weaker the SE is. In the case of Mn [Fig. 7(b)], the exchange splitting is large. The energy cost of promoting the p electron to the TM-d shell is substantial due to this large exchange splitting. Also the accepting orbital is an e_g type and is narrow in energy. These two factors will create a weak AFM SE coupling to exist in Mn.

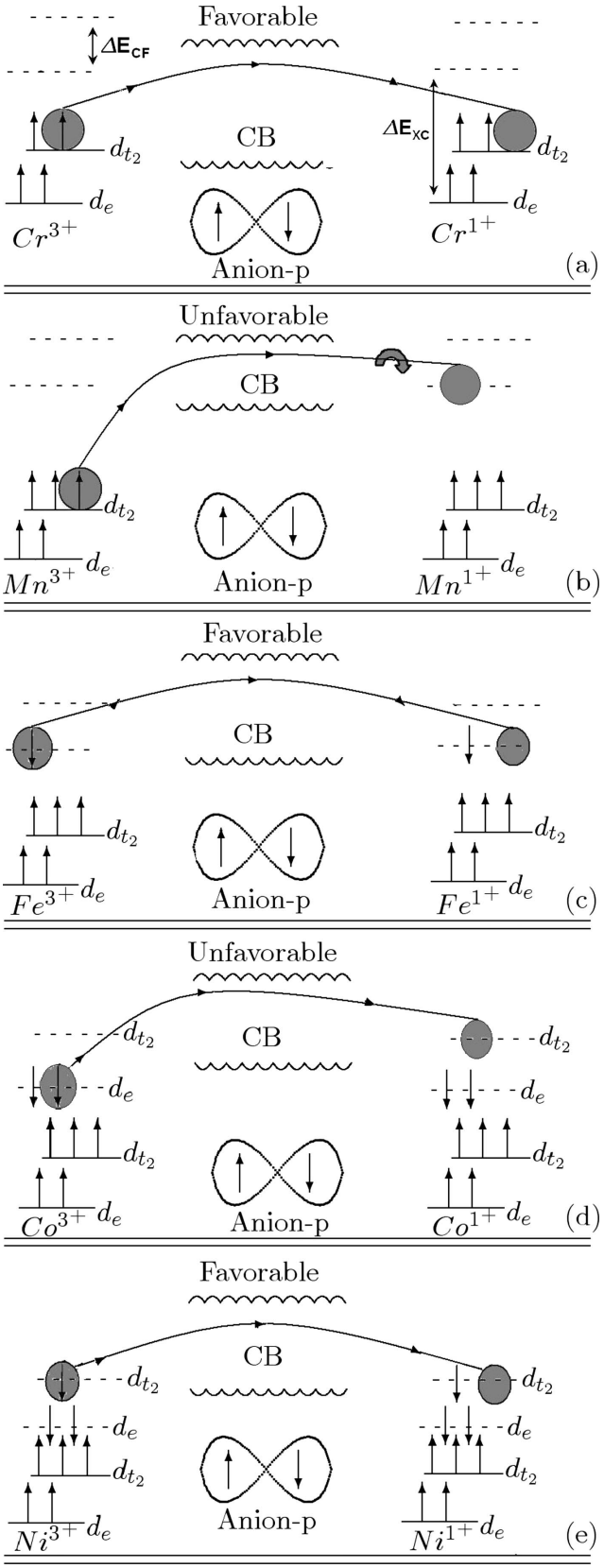

FIG. 6. Schematic of the electronic configurations for TM-cation-TM pairs under the DE mechanism, which mediates the electron transitions by requiring a FM alignment. The favorable exchanges result in half-metallic compounds.

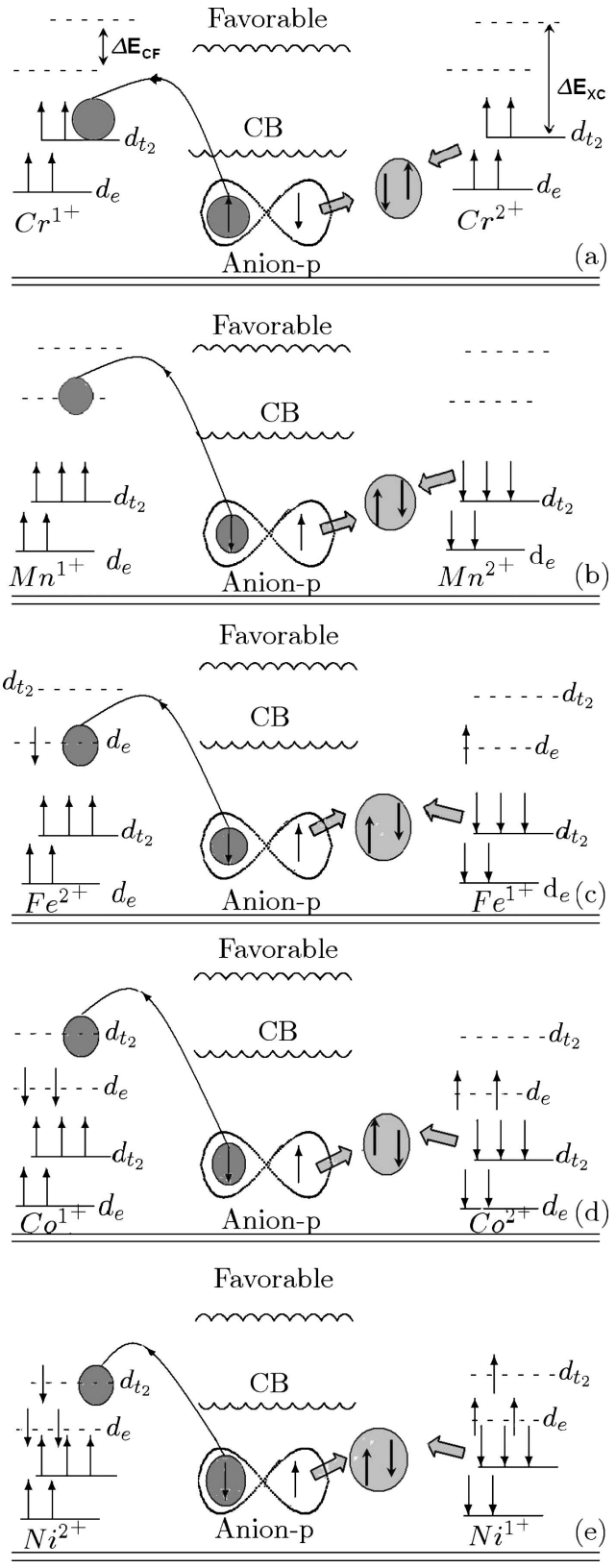

FIG. 7. Schematic of the electronic configurations for the TM-cation-TM pairs under the SE mechanism. All of the compounds (b)–(e) are required to be antiferromagnetically aligned except for Cr (a) which is required to have its spins ferromagnetically aligned in order to mediate the electronic coupling.

In Co [Fig. 7(d)] we see a shrinking exchange splitting. The promotion of the p electron must be received by the wider TM t_{2g} shell. The SE and AFM couplings are predicted to be stronger in the case of Co than in Mn given the broader width of the t_{2g} subband and energy cost of promoting the p electron.

In the case of the DMS compounds containing Cr promoting the anion's spin-up p electron is favored by maximizing S. Since the exchange splitting is large the electron will be promoted to the t_{2g} shell. The energy cost of this p-d promotion is small. Hence we should expect strong FM coupling via the SE for Cr. In the case of Fe, the energy cost of promoting the p electron to the narrow TM e_g shell is not as large as Mn, due to the smaller exchange splitting, but larger than Cr. In Fe the DE and SE couplings should be comparable yet opposite in sign to one another and may lead to an oscillatory coupling. In Ni the exchange splitting has been further reduced. In SE the p electron is transferred to the neighboring TM (left) t_{2g} shell. The energy cost in promoting this p electron is less than in any of the previous cases due to the close proximity of the TM-d peak to the VB. However, given that Ni is simultaneously involved with a strong FM DE the overall strength and sign of the magnetic coupling from this analysis is inconclusive. The strength of the AFM SE for each TM from this analysis in decreasing order is Ni, Co, Cr, Fe, and Mn.

We can see that the main difference in the p-d hybridization between the half-metallic elements Cr, Ni, and the Fe DMS is the particular d orbital that is interacting with the p orbital of the anion. This acceptor orbital has to be energetically able to acquire this electron and have significant overlap with the donor orbital. The difference between the two d suborbitals lies in the bonding geometries (Fig. 8). The d_{e_g} orbitals ($d_{x^2-y^2}$ and d_{z^2}) point along the coordinate axes, while the $d_{t_{2g}}$ orbitals (d_{xy},d_{yz}, and d_{xz}) point between the coordinate axes. These crystal geometries lead to differing amounts of suborbital overlap. Therefore, not only do we need to take into account the proximity of the TM impurities to each other but also the bonding direction. Figure 8 demonstrates how the degree of p-d suborbital overlap is determined by the bonding geometries between the TM impurities and nearest-neighbor anions.

Fe with six valence electrons has electron transitions to and from the d_{e_g} orbitals, and therefore the overlap describing the p-d interaction is between the p_x-d_{z^2} orbitals and results in a smaller overlap. The eight valence electrons of Ni provide a local moment from the electrons in the $d_{t_{2g}}$ suborbital, therefore the p-d interactions exist between the p_x-d_{xz} suborbitals and is stronger than in the case of Fe.

Lastly, Cr atoms have four valence electrons and one empty minority state in the d orbital, and the transitioning electron will travel to a $d_{t_{2g}}$ orbital on the adjacent atom, as in the case of Ni. The difference in the strength of the exchange between Ni and Cr is a consequence of the amount of the $d_{t_{2g}}$ or d_{xz} overlap with the anion's p shell. The d-shell radii of the elements have been calculated and show that as one fills up the d shell with electrons the radius of the shell shrinks.[29] The radius of a Cr d shell is roughly 30% larger than that of Ni, which explains Cr has a much larger exchange energy than Ni.

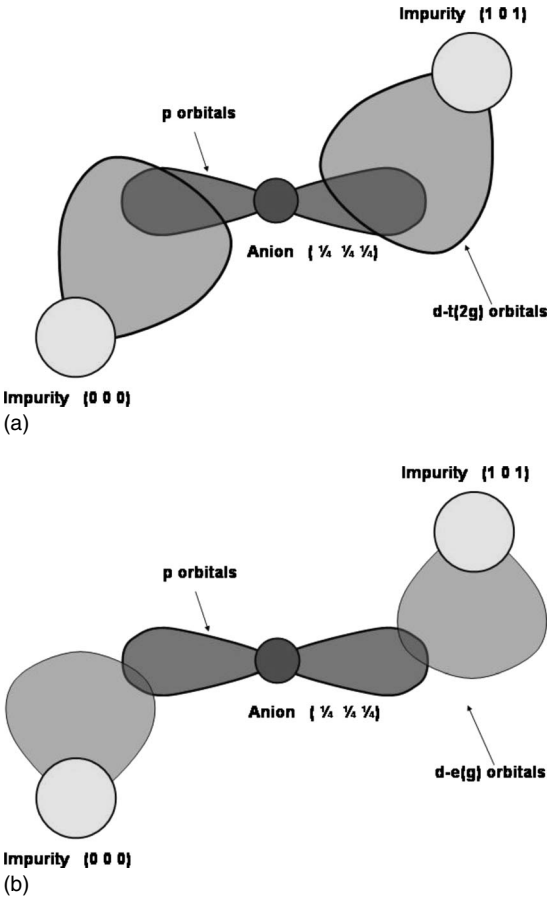

FIG. 8. Bonding directions of the p, d_{t2_g}, (left) and d_{e_g} (right) suborbitals at the closest TM spacing ($0.707L_o$). The figure is meant to display the favoritism for certain bonding orbitals pertaining to the SE mechanism.

V. RESULTS

A. Ground-state energies/exchange couplings

To determine the preferred magnetic state of a compound calculations are performed for FM and AFM configurations and the energies are compared. Intuitively, the larger the energy difference between the two states the more probable the system will exist in that magnetic GS. The calculated GS energies of the FM and AFM states for all of the DMS materials discussed in this work are shown in Fig. 9 as a function of the impurity separation distance. From the trends displayed in this figure, we can see that the only materials for which ferromagnetism is the favored state for all impurity separation distances are those which contain Cr or Ni impurities (except ZnNiTe), with Cr being more ferromagnetically stable. The compounds which contain Fe impurities exhibit an oscillatory coupling, favoring the AFM ordering at the shortest impurity spacing ($0.707L_o$) and FM ordering at subsequent impurity spacings, exhibiting behavior which is likely caused by the competing SE and DE mechanisms. The materials containing Co and Mn impurities have AFM ordering for all impurity spacings.

The exchange energy is the change in GS energy between the two magnetic configurations. The FM DMS compounds

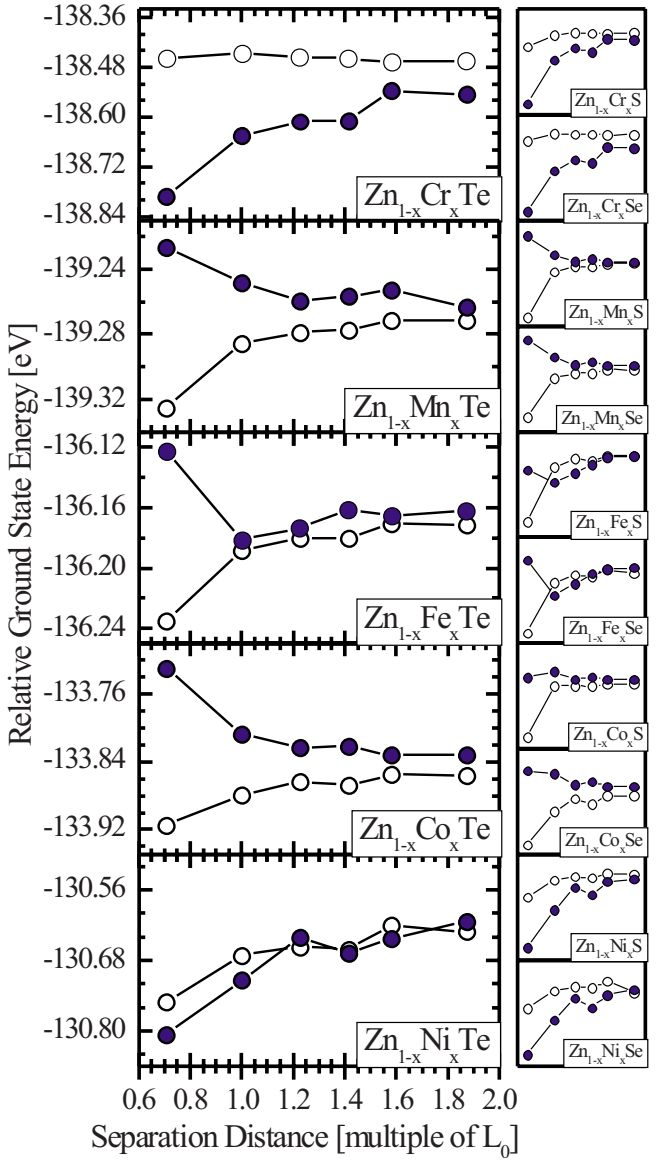

FIG. 9. (Color online) Plots showing the trends in the calculated GS energies of the doped ZnTe materials with both FM (closed circles) and AFM (open circles) ordering as a function of the impurity separation distance. The smaller plots show the GS energies for the ZnS and ZnSe materials in order to show that the response of the GS energy to the separation distance is similar for a family of anions.

are Cr and Ni. The maximum exchange energy for Cr is 0.335 eV and occurs in ZnSe. The maximum exchange energy for Ni is 0.207 eV and occurs in ZnS. The exchange energy of the calculated half-metallic materials is shown in Fig. 10 as a function of the impurity separation distance. The data displayed in this figure show that the closest impurity spacings ($0.707L_o$) yields the greatest exchange energy, which then decreases dramatically as the separation between the magnetic ions increases. This is due to a narrowing of the *d* bands as the ions are spaced further apart, and thus a smaller probability the electron will be transported in the DE and SE processes. In real samples, the statistical arrangement of the impurities would lead to a distribution of separation

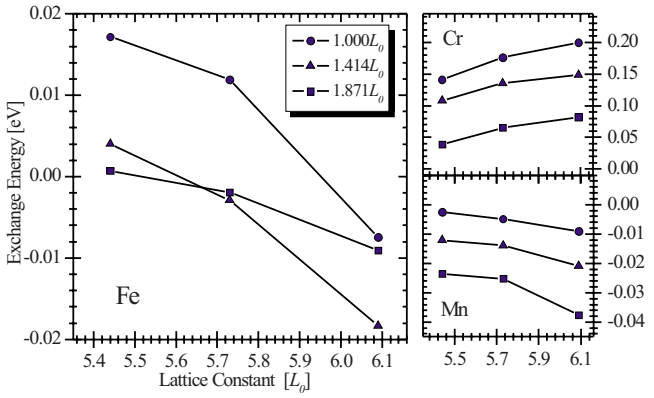

FIG. 10. (Color online) Plots showing the trends in the calculated exchange energies as a function of the impurity separation distance for the half-metallic impurities (Cr, Fe, and Ni) in ZnS, ZnSe, and ZnTe.

distances between the impurities, making the actual exchange energy a statistical averaging of the exchange distribution.

The calculated exchange energies also show a dependence on the size of the anion in the semiconducting material, as shown in Fig. 11 for ZnS, ZnSe, and ZnTe materials doped with either Cr, Mn, and Fe impurities. As the size of the anion increases so does the lattice constant. This increases the spacing between atoms. At first glance this might be expected to reduce the strength of the coupling mediated by the SE. However, the valence *p* orbitals extend out further for the larger anion. For example, the *d* orbitals of the TM series Ni→Pt→Pd broaden as you go down in the periodic table. The greater spatial extent of the *p* orbitals creates an increase of the *p-d* hybridization and thus a strengthened SE coupling.

We can verify this by examining the Cr and Mn compounds which couple strongly (Cr) and exclusively (Mn) by the SE. Figure 10 shows that the exchange energy, as expected, increases (negatively) for the Mn inset and increases (positively) for Cr with the increasing lattice constant. We investigate the effect anion size has on the strength of the DE coupling. The strength of the DE is determined by the strength of the Zener *sp-d* coupling or the weight of the impurity *d* band at the Fermi energy. The band gap is known to decrease as the size of the anion increases for the II–VI semiconductors; from Table I, S→Se→Te=2.88 eV →2.48 eV→1.86 eV thus the decreasing band gap should increase the weight of the impurity *d* band that coincides with the Fermi energy.

We address the issue of which exchange mechanism is most sensitive to the lattice constant by examining the Fe compounds which have similar coupling strengths for the SE (AFM) and DE (FM). In Fig. 11, the Fe inset shows that the exchange energy crosses the *x* axis and becomes more negative (more AFM) as the lattice constant increases. This behavior suggests that SE reduces at a slower rate as the ions spread apart than DE. Quantitatively the exchange energy will vary differently with the lattice spacing depending on the impurity and the strength and preference of each exchange coupling.

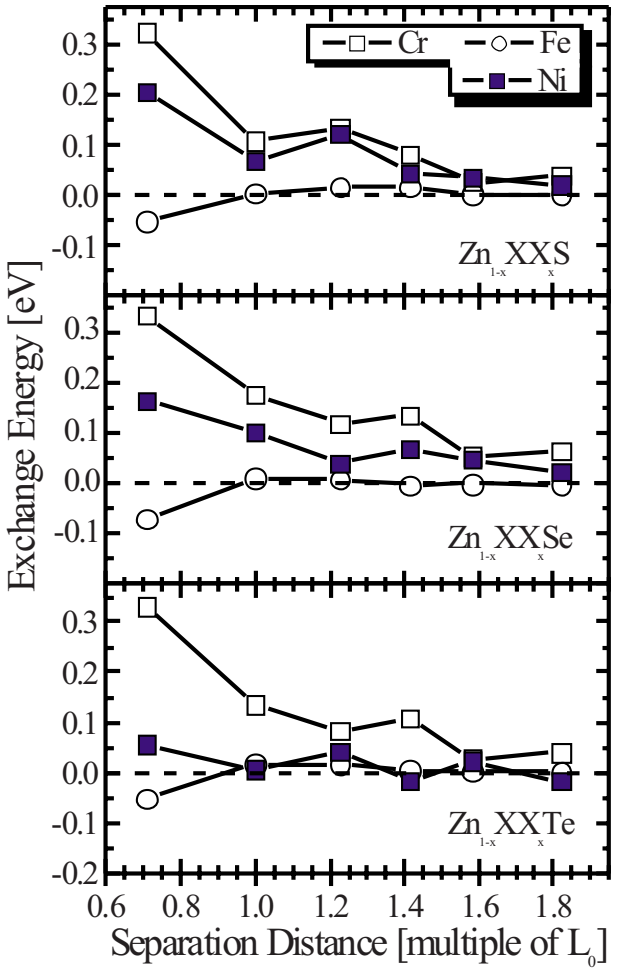

FIG. 11. (Color online) Plot showing the trend of decreasing exchange energy values as the lattice constant increases for compounds doped with Fe (left), Cr (top right), and Mn (bottom right).

In each of the compounds discussed in this work it was determined that the orientation which provided the lowest GS energy was the one in which the magnetic impurities were located closest to each other, suggesting a localization of the impurities, and their magnetic moments, inside the crystal upon its fabrication. This clustering effect may lower the Curie temperature in DMS structures, as has been shown in GaMnN systems.[30] The orientation having the shortest impurity separation distance was also found to yield the largest exchange energies of the potential orientations.

A simple calculation provides a comparative measure of the tendency of impurities to cluster by comparing the difference in the GS energy between the closest TM spacing $(0.707L_0)$ and the spacing of one lattice constant (L_0). Larger values resulting from this calculation indicate a greater inclination of the magnetic ions to cluster together.

From data presented in Fig. 12, we see that the half-metallic DMS materials, Cr and Ni, tend to cluster locally and the preference to cluster for these impurities are in the decreasing order Cr→Ni. This order of clustering strengths is similar to the strength of the magnetic exchange for these impurities. The compounds containing the impurities Cr and Ni have significant clustering strengths, while Fe has a small

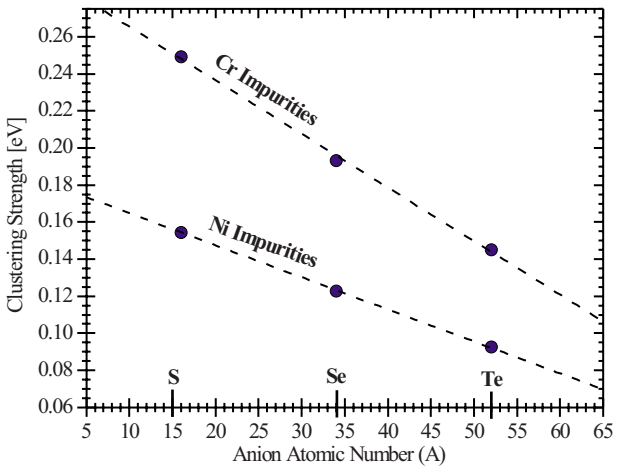

FIG. 12. (Color online) Plot showing the calculated attraction strength $[\Delta E = E_{gs}(.707L_o) - E_{gs}(1.0L_o)]$, for our Cr and Ni impurity systems as a function of the atomic number of the anion (S, Se, or Te). The trend lines indicate a linear fit to the calculated data and can be used to determine the attraction strength for other possible anions (such as oxygen).

clustering strength indicative of its oscillation between AFM and FM phases from Fig. 10. The dashed lines in Fig. 12 represent linear fits of the data for each impurity in relation to the atomic number of the compounds anion. Extrapolation of the linear fit implies that the use of smaller anion atoms leads to a stronger attraction between impurities, and therefore a more significant clustering effect of impurities in the crystal. Owing to the smaller anion, this data fit suggests that the compounds ZnCrO and ZnNiO will have large attraction strengths (0.270 and 0.170 eV, respectively), which may lead to some of the interesting characteristics discovered for ZnO DMS.[13]

This clustering effect has been previously studied for the Cr species of the ZnTe semiconductors.[18] Our results were comparable with this study on the aspect of the clustering trends that exist in these II–VI compounds. However, that study assumes that the spatial inhomogeneity of the Cr ions would automatically enhance the half-metallic property of the crystal. While that might be the case locally in the crystal the overall effect on a bulk cluster of applicable size is not so clear cut. It should be noted that our study did not take into consideration the diffusion probability of the TM ions and assumes that the energy barrier is large, given the covalent bonding potential of the DMS material.

VI. CONCLUSION

The calculated densities of states presented in this study identify two metallic impurities (Cr and Ni) which may also produce half-metallic behavior in the Zn-based II–VI DMS structures. The half-metallic behavior of Cr impurities in similar systems has been shown previously,[6,7,11,31] although the half-metallic property of Ni may require greater study.[5,7]

The other impurities studied (Mn and Co) show primarily AFM coupling, and therefore are eliminated from the possibility of being used as spin filters in spintronics. Fe-doped systems appear to exhibit a competition between the SE and

DE mechanisms, which leads to an oscillatory magnetic coupling. Whether a particular Fe sample will demonstrate a FM, AFM, or spin-glass arrangement has a strong dependence on the spatial positioning of the impurities. So then the II–VI, Zn-based, DMS compounds doped with either Cr or Ni have the greatest potential to be implemented successfully into spintronic devices

The tendency of the impurities to cluster has been established in the materials for a concentration of 4%. This clustering effect is critical for Cr based DMSs since the local ferromagnetism mediated by the SE depends greatly on the TM crystal separation/orientation. The FM ordered materials that contain Cr and Ni display this tendency to cluster the ions together. It must be considered that these impurity rich regions in the crystal could result in the FM behavior being local and not a bulk property of the crystal. Much of this work is verified by a similar study on ZnO DMS,[13] which deduced similar results.

[1] J. K. Furdyna and J. Kossut, *Diluted Magnetic Semiconductors* (Academic, New York, 1988), Vol. 25.
[2] J. K. Furdyna, J. Appl. Phys. **64**, R29 (1988).
[3] J. K. Furdyna, J. Appl. Phys. **53**, 7637 (1982).
[4] C. M. Fang, G. A. Wijs, and R. A. Groot, J. Appl. Phys. **91**, 8340 (2002).
[5] R. A. Stern and T. M. Schuler, J. Appl. Phys. **95**, 7468 (2004).
[6] J. Blinowski, P. Kacman, and J. A. Majewski, Phys. Rev. B **53**, 9524 (1996).
[7] K. Sato, H. Katayama-Yoshida, S. Yamagata, Y. Suzuki, and K. Ando, Phys. Status Solidi B **229**, 673 (2002).
[8] H. Saito and W. Zayets, J. Appl. Phys. **91**, 8085 (2002).
[9] W. Mac, A. Twardowski, P. J. T. Eggenkamp, H. J. M. Swagten, Y. Shapira, and M. Demianiuk, Phys. Rev. B **50**, 14144 (1994).
[10] L. M. Sandratskii and P. Bruno, J. Phys.: Condens. Matter **15**, 585 (2003).
[11] H. Saito, V. Zayets, S. Yamagata, and K. Ando, J. Appl. Phys. **93**, 6796 (2003).
[12] T. M. Pekarek, D. J. Arenas, B. C. Crooker, I. Miotkowski, and A. K. Ramdas, J. Appl. Phys. **95**, 7178 (2004).
[13] L. M. Sandratskii and P. Bruno, Phys. Rev. B **73**, 045203 (2006).
[14] L. M. Sandratskii, Phys. Rev. B **68**, 224432 (2003).
[15] T. M. Schuler, R. A. Stern, R. McNorton, S. D. Willoughby, J. M. MacLaren, D. L. Ederer, V. Perez-Dieste, F. J. Himpsel, S. A. Lopez-Rivera, and T. A. Callcott, Phys. Rev. B **72**, 045211 (2005).
[16] A. Twardowski, J. Appl. Phys. **67**, 5108 (1990).
[17] Y. Uspenskii, E. Kulatov, H. Mariette, H. Nakayama, and H. Ohta, J. Magn. Magn. Mater. **258**, 248 (2003).
[18] Y. Gou, J. Cao, X. S. Chen, and W. Lu, Solid State Commun. **138**, 275 (2006).
[19] C. Zener, Phys. Rev. **81**, 440 (1951).
[20] P. W. Anderson, Phys. Rev. **79**, 350 (1950).
[21] M. Gorska and J. R. Anderson, Phys. Rev. B **38**, 9120 (1988).
[22] P. M. Krstajic, F. M. Peeters, V. A. Ivanov, V. Fleurov, and K. Kikoin, Phys. Rev. B **70**, 195215 (2004).
[23] G. Kresse and J. Furthmuller, Vienna *ab-initio* simulation package, 2001, http://cms.mpi.univie.ac.at/vasp/
[24] P. E. Blochl, Phys. Rev. B **50**, 17953 (1994).
[25] G. Kresse and D. Joubert, Phys. Rev. B **59**, 1758 (1999).
[26] J. P. Perdew, *Electronic Structure of Solids '91* (Akademie, Berlin, 1991).
[27] S. H. Vosko, L. Wilk, and M. Nusair, Can. J. Phys. **58**, 1200 (1980).
[28] P. W. Anderson, Phys. Rev. **115**, 2 (1959).
[29] V. L. Moruzzi, J. F. Janak, and A. R. Williams, *Calculated Electronic Properties of Metals* (Pergamon, New York, 1978).
[30] L. M. Sandratskii, P. Bruno, and S. Mirbt, Phys. Rev. B **71**, 045210 (2005).
[31] L. M. Sandratskii and P. Bruno, J. Phys.: Condens. Matter **15**, L585 (2003).